ChemComm

COMMUNICATION

View Article Online
View Journal | View Issue

Cite this: *Chem. Commun.*, 2014, **50**, 11492

Received 20th June 2014,
Accepted 7th August 2014

DOI: 10.1039/c4cc04713c

www.rsc.org/chemcomm

Dual effect of thiol addition on fluorescent polymeric micelles: ON-to-OFF emissive switch and morphology transition†

Anne B. Mabire,[a] Mathew P. Robin,[a] Helen Willcock,[a] Anaïs Pitto-Barry,[a] Nigel Kirby[b] and Rachel K. O'Reilly*[a]

The morphology transition from micelles to vesicles of a solution-state self-assembled block copolymer, containing a fluorescent dye at the core–shell interface, has been induced by an addition–elimination reaction using a thiol, and has been shown to be coupled to a simultaneous ON-to-OFF switch in particle fluorescence.

Precise control over solution-state self-assembled polymer morphologies is currently of great interest to the research community. Various morphologies such as spherical micelles, cylinders, rods and vesicles can be formed by the self-assembly of amphiphilic block copolymers in selective solvents.[1] Block copolymer composition and properties control the morphology that is adopted in solution by the amphiphile. Conventional self-assembled morphologies are based on hydrophilic–hydrophobic repulsive interactions,[2] and as a result, self-assembled nanostructures formed from stimuli-responsive polymers are able to undergo morphology transitions induced by external stimuli such as pH, temperature and light.[3–9] Importantly, the responsive behavior of self-assemblies enables these new materials to find applications in nanotechnology and/or drug delivery.[10–15] Moreover, self-assembled nanostructures having fluorescent properties are also of interest given the desire to track such species in applications such as nanomedicine.[16–18]

Previously, Baker *et al.* have shown that the conversion of dibromomaleimide (DBM) to dithiomaleimide (DTM) is highly efficient, and that by an excess of thiol further conversions can occur due to retention of the double bond in the DTM motif.[19] Furthermore, we previously reported that DTM's functionalized with alkyl thiols are highly fluorescent whilst those with aromatic substituents show a significant decrease in fluorescence emission.[20] Recently, we demonstrated that the DTM motif can be introduced into block copolymers as a highly emissive fluorescent self-reporting probe *via* a dual ring-opening polymerization and reversible addition-fragmentation chain transfer polymerization (ROP/RAFT) initiator.[20] Aqueous solution-state self-assembly of these amphiphilic block copolymers results in DTM incorporation at the core–shell interface of spherical micelles.[21] Herein, we utilize the reactivity of the DTM group to induce a morphology transition from spherical micelles to vesicles which occurs simultaneously with an ON-to-OFF switch of fluorescence emission (Fig. 1). The change in fluorescence and morphology is induced by an addition–elimination reaction which removes the hydrophobic segment that is connected to the DTM functional group at the block copolymer interface, and replaces it with an aromatic substituent. This subtle change in chemistry of the DTM group has a significant effect on the properties of the assembly. We propose the use of this triggered change in fluorescence and overall self-assembled structure at the DTM group as an accessible read-out for the change in chemistries within a block copolymer in a polymeric nanostructure. As such we propose this approach has interesting potential scope for use in sensing and also tracking applications.

We first synthesized an amphiphilic block-dye-block copolymer *via* a combination of ROP[22] and RAFT polymerization[23] utilizing a dual ROP/RAFT initiator, **1** (Scheme 1). The design of this initiator species ensures that the DTM group is located between

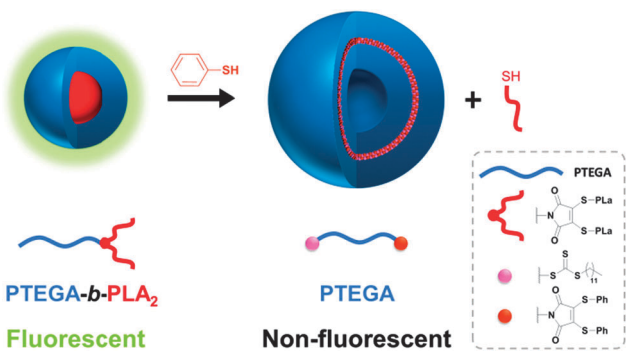

Fig. 1 Schematic of the morphology change induced by an addition–elimination reaction of the micelle with thiophenol.

[a] *Department of Chemistry, University of Warwick, Coventry, CV4 7AL, UK. E-mail: r.k.o-reilly@warwick.ac.uk; Tel: +44 (0)247 652 3236*
[b] *Australian Synchrotron, 800 Blackburn Road, Clayton, Victoria 3168, Australia*

† Electronic supplementary information (ESI) available. See DOI: 10.1039/c4cc04713c

the hydrophobic and the hydrophilic blocks, allowing the addition–elimination reaction to be coupled with both a morphology transition and a fluorescence ON-to-OFF switch. The structure and properties of the amphiphilic copolymers were carefully chosen to enable a significant modification of the hydrophilic/hydrophobic balance alongside a fluorescence emission decrease by changing the nature of the hydrophobic segment. As the hydrophobic segments were connected to the DTM motif as the thiol ligands, subsequent addition–elimination with a thiol following self-assembly would allow elimination of the hydrophobic blocks.

The DTM-containing ROP/RAFT dual initiator, **1**, was synthesized from a 2,3-DBM-functionalized RAFT agent.[24] Reaction with mercaptoethanol and triethylamine gives a fluorescent DTM-functionalized ROP/RAFT dual initiator (**1**) with two hydroxyl groups allowing ROP[22] of *rac*-lactide to be performed to afford polymer **1′**. This polymer was then chain-extended to afford the diblock copolymer [poly(triethyleneglycol monomethyl ether methacrylate)]-*b*-[poly(D,L-lactide)]$_2$, **2**, see Scheme 1. The well-defined fluorescent block-dye-block copolymer, PTEGA-*b*-PLA$_2$, **2**, was fully characterized using NMR spectroscopy and SEC analysis (M_n (NMR) = 33.1 kDa, M_n (SEC, DMF) = 19.5 kDa, $Đ_M$ = 1.42).

The self-assembly of copolymer, **2**, into micelles, **3**, was achieved *via* direct dissolution of the copolymer in purified 18.2 MΩ cm water at a concentration of 1 mg mL^{-1}. The fluorescence spectra of the spherical micelles **3** in 18.2 MΩ cm water shows an excitation maxima at 405 nm, and an emission maxima at 510 nm, which are similar to previously reported DTM polymer systems.[21] The size and morphology of the micelles was confirmed by light scattering and microscopy analysis. Multi-angle laser light scattering (MA-LLS) indicated R_h = 26 nm (see ESI†) and dry-state transmission electron microscopy (TEM) analysis on graphene oxide, a very thin support that does not require staining, suggests a spherical morphology, see Fig. 2a.[25]

The micelle solution, **3**, was treated with 20 equiv. of thiophenol, and then purified by exhaustive dialysis (MWCO = 1 kDa). Further experiments with a range of aromatic thiols indicated that the reaction also works efficiently with a small excess of thiol. The thiol underwent addition to the DTM group, with corresponding elimination to afford thio-terminated poly(*rac*-lactide), **7**. Given that the thio-PLA residue is insoluble in water, the solution was then centrifuged to remove the thio-PLA precipitate (see ESI† for ^{1}H NMR spectrum).

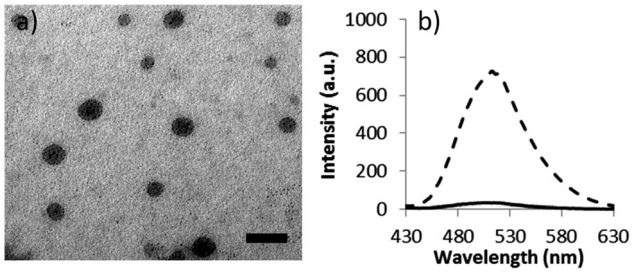

Fig. 2 (a) Representative unstained TEM image of micelles (scale bar = 50 nm) **3** and (b) fluorescence emission spectra before (dash line) and after the reaction (solid line), with excitation at 405 nm.

To characterize the particle morphology of assembly **4a**, Multi-Angle Laser Light Scattering (MA-LLS) was performed to determine the radius of gyration R_g and hydrodynamic radius R_h of the assemblies, **4a**. The ratio of R_g/R_h gives an indication of the nanostructure morphology, with 0.775 indicating a solid micelle and 1 indicating a hollow vesicular structure.[26] By interpreting the data collected in static light scattering (SLS) mode, using CONTIN analysis, the radius of gyration R_g was determined to be 51 nm. From the dynamic light scattering (DLS) data, R_h was found to be 56 nm. For nanostructure **4a** the R_g/R_h was calculated to be 0.91, which suggests that nanostructures formed are hollow vesicular particles (see ESI†). We propose that the vesicles' hydrophobic layer is composed of both the substituted maleimide group (containing the –SPh ligands) and dodecyl end group (the RAFT agent Z-group). This is consistent with previous reports which have shown that hydrophilic polymers with hydrophobic aromatic and aliphatic end-groups can self-assemble into nanoparticles, including vesicles.[27–30]

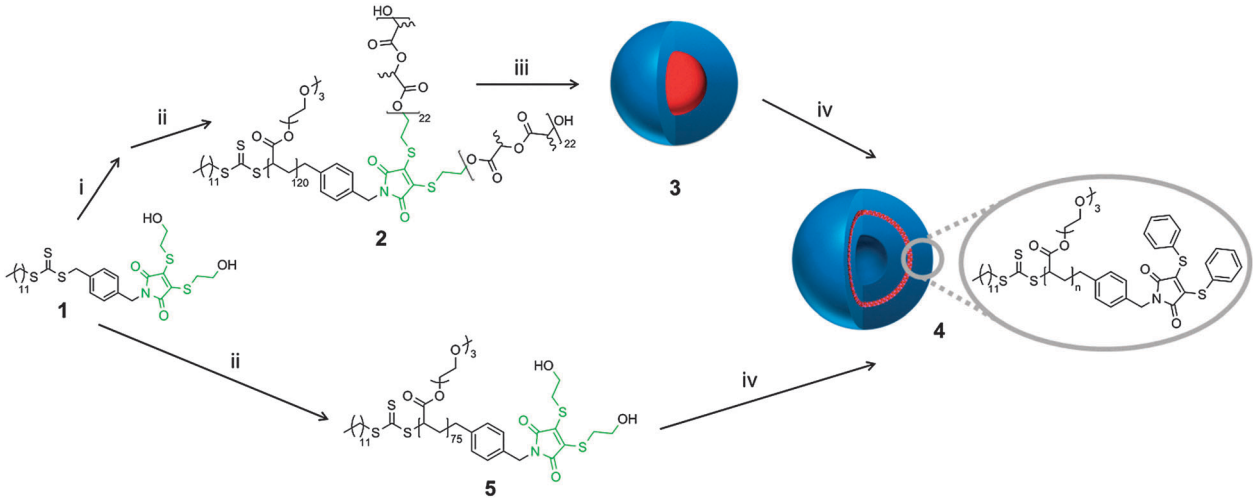

Scheme 1 Preparation of polymers **2** and **5** from CTA **1**, preparation of micelles **3**, and the addition–elimination reaction of **3** and **5** which results in a morphology transition to afford vesicle **4**. Conditions: (i) *rac*-lactide, thiourea, (−)-sparteine, CH_2Cl_2; (ii) AIBN, $CHCl_3$, TEGA at 60 °C; (iii) direct dissolution in water; (iv) thiophenol.

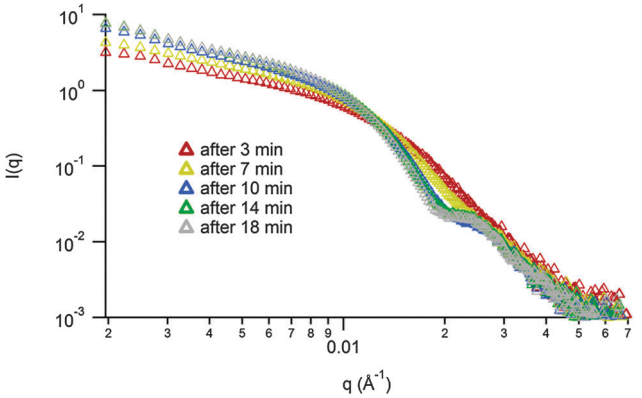

Fig. 3 SAXS profiles for the *in situ* micelle-to-vesicle transition.

Moreover, examination of the emission spectrum of the resultant solution of **4a** indicated a drastic decrease of the fluorescence as a consequence of the modification at the DTM reactive center. At the same excitation wavelength, the comparison of the emission spectra of the solution before and after the reaction (measured at the same concentration) showed a decrease in the intensity of the maxima (510 nm) from 730 to 30 a.u., see Fig. 2b.

Unfortunately, attempts to image the vesicles by dry-state TEM were not possible as the nanostructures were not stable to dehydration. However, to further probe the proposed micelle-to-vesicle transition upon thiol addition synchrotron SAXS experiments were performed. The transition described in Scheme 1 part (iv) was performed in the beamline and the *in situ* kinetics of the morphology transition were examined (Fig. 3). This has the advantage that it allows for the monitoring of the transition without the need for removal of insoluble PLA, drying and suspension of the nanostructures (as was necessary for MA-LLS analysis). Analysis of the SAXS curves over a 20 minute time period indicates a change of morphology. At the beginning, a spherical morphology was observed. An increase in the size of the morphologies in solution happened promptly (less than 10 min) and a form factor fit indicated the formation of vesicles as well as the presence of random chains in solution (thio-PLA in solution) (see ESI† for the different fittings of the SAXS curves over time).

To further probe the vesicle formation which was observed in the transition from **3** to **4a**, the addition–elimination reaction was performed on a range of model homopolymers (data shown for PTEGA$_{75}$, M_n (NMR) = 16.2 kDa, M_n (SEC) = 13.5 kDa, $Đ_M$ = 1.19), **5**, synthesized *via* RAFT polymerization of TEGA utilizing **1** as a chain transfer agent (CTA). DLS analysis of aqueous solutions of the initial homopolymer **5** (which possesses α-diol and ω-dodecyl end-groups), indicated the presence of unimers in solution. However, after the addition–elimination reaction between **5** and an excess of thiophenol, well-defined nanostructures were observed, **4b**. MA-LLS was performed, and values of R_g and R_h were extracted from the results. By interpreting the data collected in SLS mode, the R_g equals 63 nm and from the DLS data, the R_h equals 68 nm and hence the R_g/R_h obtained was 0.93, which once again suggests that the nanostructures formed in this reaction are vesicles. Similar to particles **4a** which result from reaction of the micelles (**3**) with thiophenol, the reaction of the homopolymer **5** with thiophenol forms particles **4b** of a similar size and morphology. This is understandable as the addition–elimination reaction of **3** and **5** would be expected to give the same resultant homopolymer, namely P(TEGA) homopolymer with α-SPh and ω-dodecyl end-groups, which would be expected to assemble into a similar morphology. As observed for the addition–elimination reaction with the micelles, the fluorescence emission of the homopolymer solution again underwent a fast (15 min by analysis of the 535 nm emission) ON-to-OFF switch during the reaction with thiophenol, see ESI.†

In conclusion, we have shown that an amphiphilic block-dye-block copolymer containing a DTM group can undergo a fast morphology transition from spherical micelles to vesicles. This is triggered by the addition of thiophenol to the DTM group, with corresponding elimination of the hydrophobic blocks. A unimer-to-vesicle transition also occurs for a DTM group-containing homopolymer. In both cases addition of thiophenol leads to a simultaneous fluorescence ON-to-OFF switch. This approach is extremely versatile and could be tuned for utilization with a range of aromatic thiols and self-assembled systems which contain the DTM functional group. We suggest that such a simultaneous ON–OFF switch and morphological reorganization could be readily applied as a tracking ingmechanism and also as a mechanism for monitoring release in biological and/or synthetic self-assembled systems.

We are thankful to the EPSRC and the IAS at the University of Warwick for funding. Equipment used in this research was funded in part through Advantage West Midlands (AWM) Science City Initiative and in part by the ERDF. We acknowledge Professor Andrew Dove and Dr Tara Schiller for assistance with the SAXS measurements and Mr Daniel Wright for assistance with MA-LLS analysis.

Notes and references

1 Y. Mai and A. Eisenberg, *Chem. Soc. Rev.*, 2012, **41**, 5969–5985.
2 A. Blanazs, S. P. Armes and A. J. Ryan, *Macromol. Rapid Commun.*, 2009, **30**, 267–277.
3 A. O. Moughton and R. K. O'Reilly, *Chem. Commun.*, 2010, **46**, 1091–1093.
4 J.-Z. Du, H.-Y. Long, Y.-Y. Yuan, M.-M. Song, L. Chen, H. Bi and J. Wang, *Chem. Commun.*, 2012, **48**, 1257–1259.
5 A. Klaikherd, C. Nagamani and S. Thayumanavan, *J. Am. Chem. Soc.*, 2009, **131**, 4830–4838.
6 C. L. McCormick, B. S. Sumerlin, B. S. Lokitz and J. E. Stempka, *Soft Matter*, 2008, **4**, 1760–1773.
7 F. Chécot, S. Lecommandoux, Y. Gnanou and H.-A. Klok, *Angew. Chem., Int. Ed.*, 2002, **41**, 1339–1343.
8 C. Chang, H. Wei, J. Feng, Z.-C. Wang, X.-J. Wu, D.-Q. Wu, S.-X. Cheng, X.-Z. Zhang and R.-X. Zhuo, *Macromolecules*, 2009, **42**, 4838–4844.
9 W. Kim, J. Thévenot, E. Ibarboure, S. Lecommandoux and E. L. Chaikof, *Angew. Chem., Int. Ed.*, 2010, **49**, 4257–4260.
10 M. Lazzari and M. A. López-Quintela, *Adv. Mater.*, 2003, **15**, 1583–1594.
11 G. Gaucher, M.-H. Dufresne, V. P. Sant, N. Kang, D. Maysinger and J.-C. Leroux, *J. Controlled Release*, 2005, **109**, 169–188.
12 Z. L. Tyrrell, Y. Shen and M. Radosz, *Prog. Polym. Sci.*, 2010, **35**, 1128–1143.
13 K. Miyata, R. J. Christie and K. Kataoka, *React. Funct. Polym.*, 2011, **71**, 227–234.
14 E. G. Kelley, J. N. L. Albert, M. O. Sullivan and T. H. Epps, III, *Chem. Soc. Rev.*, 2013, **42**, 7057–7071.

15 M. Elsabahy and K. L. Wooley, *Chem. Soc. Rev.*, 2012, **41**, 2545–2561.
16 M. J. Ruedas-Rama, J. D. Walters, A. Orte and E. A. H. Hall, *Anal. Chim. Acta*, 2012, **751**, 1–23.
17 F. Canfarotta, M. J. Whitcombe and S. A. Piletsky, *Biotechnol. Adv.*, 2013, **31**, 1585–1599.
18 S. M. Janib, A. S. Moses and J. A. MacKay, *Adv. Drug Delivery Rev.*, 2010, **62**, 1052–1063.
19 M. E. B. Smith, F. F. Schumacher, C. P. Ryan, L. M. Tedaldi, D. Papaioannou, G. Waksman, S. Caddick and J. R. Baker, *J. Am. Chem. Soc.*, 2010, **132**, 1960–1965.
20 M. P. Robin, P. Wilson, A. B. Mabire, J. K. Kiviaho, J. E. Raymond, D. M. Haddleton and R. K. O'Reilly, *J. Am. Chem. Soc.*, 2013, **135**, 2875–2878.
21 M. P. Robin, A. B. Mabire, J. C. Damborsky, E. S. Thom, U. H. Winzer-Serhan, J. E. Raymond and R. K. O'Reilly, *J. Am. Chem. Soc.*, 2013, **135**, 9518–9524.
22 R. C. Pratt, B. G. G. Lohmeijer, D. A. Long, P. N. P. Lundberg, A. P. Dove, H. Li, C. G. Wade, R. M. Waymouth and J. L. Hedrick, *Macromolecules*, 2006, **39**, 7863–7871.
23 G. Moad, E. Rizzardo and S. H. Thang, *Aust. J. Chem.*, 2009, **62**, 1402–1472.
24 M. P. Robin, M. W. Jones, D. M. Haddleton and R. K. O'Reilly, *ACS Macro Lett.*, 2012, **1**, 222–226.
25 J. P. Patterson, A. M. Sanchez, N. Petzetakis, T. P. Smart, T. H. Epps, III, I. Portman, N. R. Wilson and R. K. O'Reilly, *Soft Matter*, 2012, **8**, 3322–3328.
26 J. P. Patterson, M. P. Robin, C. Chassenieux, O. Colombani and R. K. O'Reilly, *Chem. Soc. Rev.*, 2014, **43**, 2412–2425.
27 J. Du, H. Willcock, J. P. Patterson, I. Portman and R. K. O'Reilly, *Small*, 2011, **7**, 2070–2080.
28 J. Xu, L. Tao, C. Boyer, A. B. Lowe and T. P. Davis, *Macromolecules*, 2010, **44**, 299–312.
29 J. P. Patterson, E. G. Kelley, R. P. Murphy, A. O. Moughton, M. P. Robin, A. Lu, O. Colombani, C. Chassenieux, D. Cheung, M. O. Sullivan, T. H. Epps, III and R. K. O'Reilly, *Macromolecules*, 2013, **46**, 6319–6325.
30 T. Liu, W. Tian, Y. Zhu, Y. Bai, H. Yan and J. Du, *Polym. Chem.*, 2014, **5**, 5077–5088.

Electronic Supplementary Material (ESI) for ChemComm.

Supporting Information

for

Dual effect of thiol addition on fluorescent polymeric micelles: ON-to-OFF switch and morphology transition

Anne B. Mabire [a], Mathew P. Robin [a], Helen Willcock [a], Anais Pitto-Barry [a], Nigel Kirby [b] and Rachel K. O'Reilly[a]*

[a] *Department of Chemistry, Library Road, University of Warwick, Coventry, CV4 7AL, UK. E-mail: r.k.o-reilly@warwick.ac.uk*

[b] *Australian Synchrotron, 800 Blackburn Road, Clayton, Victoria 3168, Australia*

I. Experimental

Materials and apparatus

Chemicals were used as received from Aldrich, Fluka and Acros. Dry solvents were obtained by passing over a column of activated alumina using an Innovative Technologies solvent purification system. TEGA was synthesized as previously reported and stored below 4 °C.[1] CTA, **1** and PLA_2, **1'**, were prepared as previously reported.[2, 3]

^1H and ^{13}C NMR spectra were recorded on a Bruker DPX-400 spectrometer in $CDCl_3$. Chemical shifts are given in ppm downfield from the internal standard tetramethylsilane (TMS). Size exclusion chromatography (SEC) measurements were conducted using a Varian 390-LC-Multi detector suite fitted with differential refractive index (DRI), light scattering (LS) and photodiode array (PDA) detectors equipped with a guard column (Varian Polymer Laboratories PLGel 5 μm, 50×7.5 mm) and two mixed D columns (Varian Polymer Laboratories PLGel 5 μm, 300×7.5 mm). The mobile phase was either tetrahydrofuran (THF) with 2% triethylamine (TEA) or dimethylformamide (DMF) with 5 mmol NH_4BF_4 at 50 ^oC operating at a flow rate of 1.0 mL·min^{-1} and data was analyzed using Cirrus v3.3 with calibration curves produced using Varian Polymer laboratories Easi-Vials linear poly(styrene) or poly(methyl)methacrylate standards. Multi-angle Laser Light Scattering measurements were performed at angles of observation ranging from 30° up to 150° with an ALV CGS3 setup operating at λ_0 = 632nm and at 25°C ± 1°C, the data was collected with 100s run time in duplicate unless otherwise specified. Calibration was achieved with filtered toluene and the background was measured with 18.2 MΩ.cm water. Electric field autocorrelation functions ($g_1(q,t)$) were fitted with CONTIN. Synchrotron small-angle X-ray scattering (SAXS) measurements were carried on the SAXS/WAXS beamline at the Australian Synchrotron facility at a photon energy of 11 keV. The samples in solution were run by using a 1.5 mm diameter quartz capillary. Temperature was held at 25 °C and controlled *via* a water bath connected to a brass block which is part of the sample holder. The measurements were collected at a sample to detector distance of 7.323 m to give a q range of 0.02 to 0.14 Å^{-1}, where q is the scattering vector and is related to the scattering angle (2θ) and the photon wavelength (λ) by the following equation:

$$q = \frac{4\pi \, sin(\theta)}{\lambda}$$

All patterns were normalised to fixed transmitted flux using a quantitative beamstop detector. The scattering from a blank was measured in the same capillary and was subtracted for each

measurement. The two-dimensional SAXS images were converted in one-dimensional SAXS profile (*I(q) versus q*) by circular averaging, where *I(q)* is the scattering intensity. The functions used for the fitting from the NIST SANS analysis package were "Guinier-Porod",[4, 5] "Debye",[6] "PolyCoreForm"[7] and "Debye".[6] ScatterBrain[8] and Igor[9] were used to plot and analyse the data. The scattering length density of the solvent and the monomers were calculated using the "Scattering Length Density Calculator"[10] provided by NIST Center for Neutron Research. Limits for *q* range were applied for the fittings from 0.002 to 0.1 $Å^{-1}$. Solutions of graphene oxide were synthesised as reported previously.[10a] Aqueous solutions of graphene oxide (0.10 mg mL^{-1}) were sonicated for 30 s prior to use. Lacey carbon grids (400 Mesh, Cu) (Agar Scientific) were cleaned using air plasma from a glow-discharge system (2 min, 20 mA). The TEM grids were placed on a filter paper and one drop (≈ 0.08 mL) of the sonicated GO solution was deposited onto each grid from a height of ≈ 1 cm, allowing the filter paper to absorb the excess solution, and the grids were left to air-dry in a dessicator cabinet for ≈ 60 min. 4 μL of the nanoparticle dispersion (~20 ppm) was pipetted onto a GO grid and left to air-dry in a dessicator cabinet for ≈ 60 min. Brightfield TEM images were captured with a transmission electron microscope (JEOL TEM-2011), operating at 200 kV. Fluorescence spectra were recorded using a Perkin-Elmer LS 55 Fluorescence Spectrometer.

Synthetic protocols

The block copolymer PTEGA-*b*-PLA_2, **2**, has been synthesised as previously reported.[3]

*Self-assembly of PTEGA-b-PLA_2 micelles, **3***

The self-assembly of copolymer, **2,** into micelles, **3,** was performed by direct dissolution of **2** in 18.2 MΩ.cm water at concentrations of 0.5 $mg.mL^{-1}$, 1 $mg.mL^{-1}$ and 2 $mg.mL^{-1}$.

Addition-Elimination reaction with PTEGA-b-PLA_2 micelles

20 equivalents of thiophenol were added to **3**. The reaction was stirred at room temperature for 1 h. The mixture was purified *via* exhaustive dialysis (MWCO = 1000 Da) against 18.2 MΩ.cm water to remove the excess thiophenol, centrifuged to separate the precipitate (**6**) and freeze-dried. The resultant solid was resuspended at 1 $mg.mL^{-1}$ to give a solution of vesicles (**4a**).

Addition-Elimination reaction with PTEGA homopolymer

Polymer **5** was dissolved in 18.2 MΩ.cm water at 1 mg/mL and 20 equivalents of thiophenol were added to the solution. The reaction was stirred at room temperature for 1 h. The mixture was purified *via* exhaustive dialysis (MWCO = 1000 Da) against 18.2 MΩ.cm water to remove the excess of thiophenol and freeze-dried. The resultant solid was resuspended at 1 $mg.mL^{-1}$ to give a solution of vesicles (**4b**).

II. Characterisation data

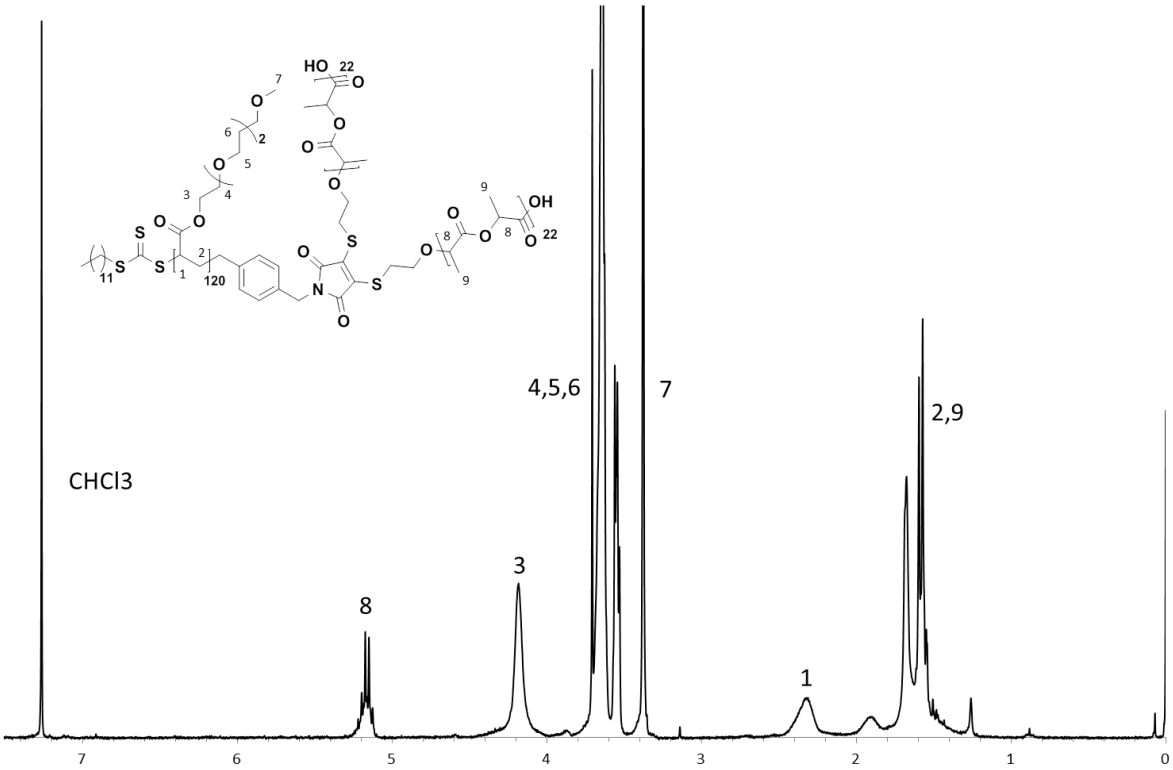

Figure S1. ^{1}H NMR (400 MHz, $CDCl_3$) spectrum of PTEGA-*b*-PLA_2, **2**.

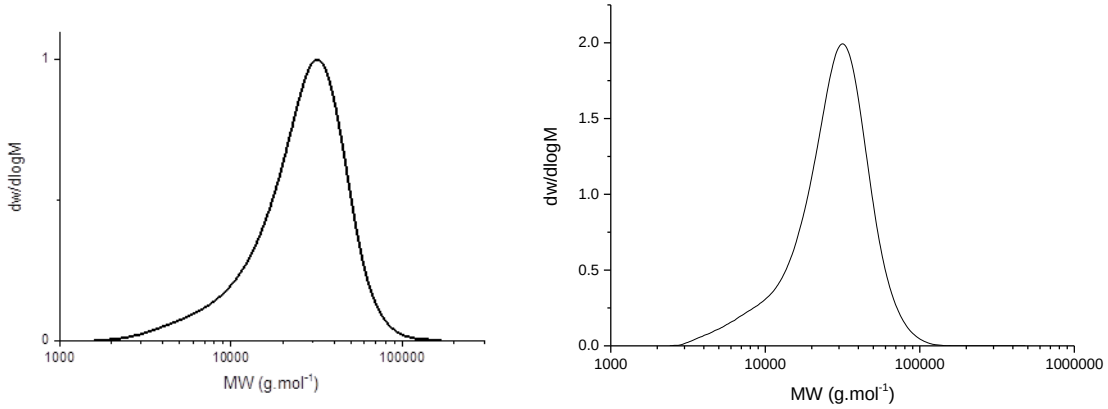

Figure S2. Molecular weight distribution obtained by SEC, LHS: using polystyrene calibration and THF as the eluent and RHS using polymethylmethacrylate calibration and DMF as the eluent for the block copolymer PTEGA-b-PLA2, **2**.

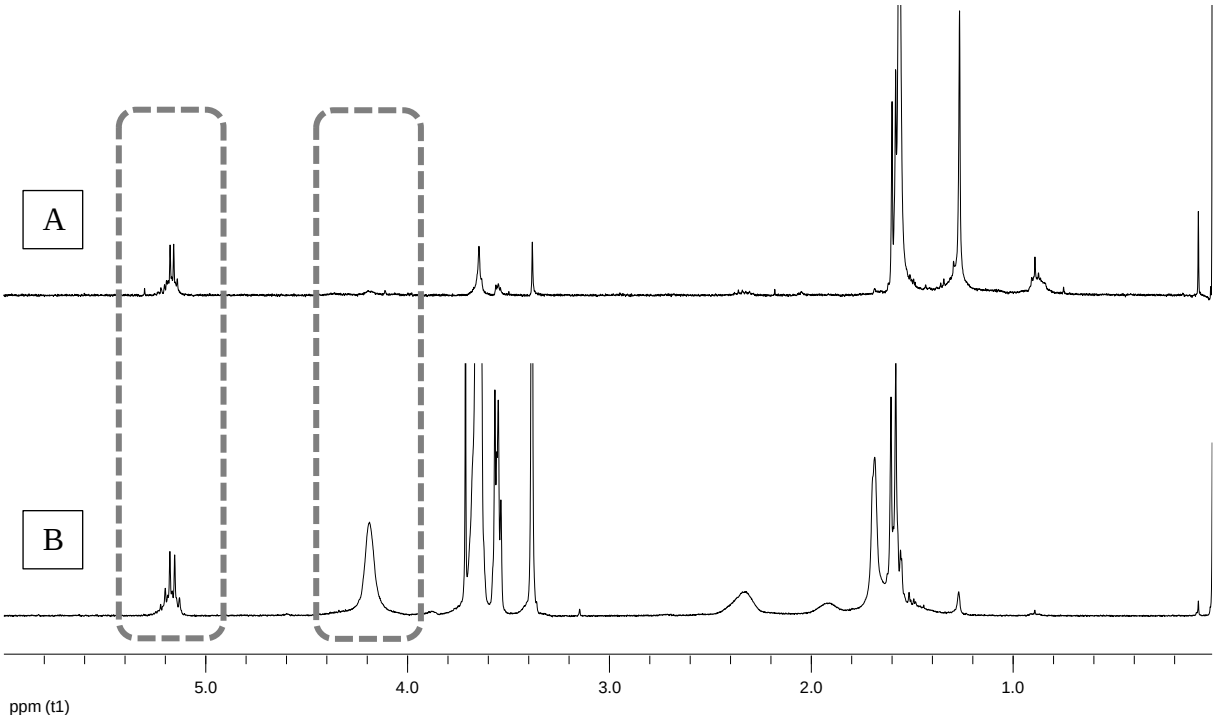

Figure S3. (A) ^{1}H NMR (400 MHz, $CDCl_3$) spectrum of the thio-PLA, **6**, obtained after separation following the addition-elimination reaction compared to (B) ^{1}H NMR (400 MHz, $CDCl_3$) spectrum of block copolymer PTEGA-*b*-PLA_2, **2** in $CDCl_3$. Highlighting the presence of the characteristic PLA signal at 5.2 ppm and the absence of characteristic TEGA signal at 4.2 ppm.

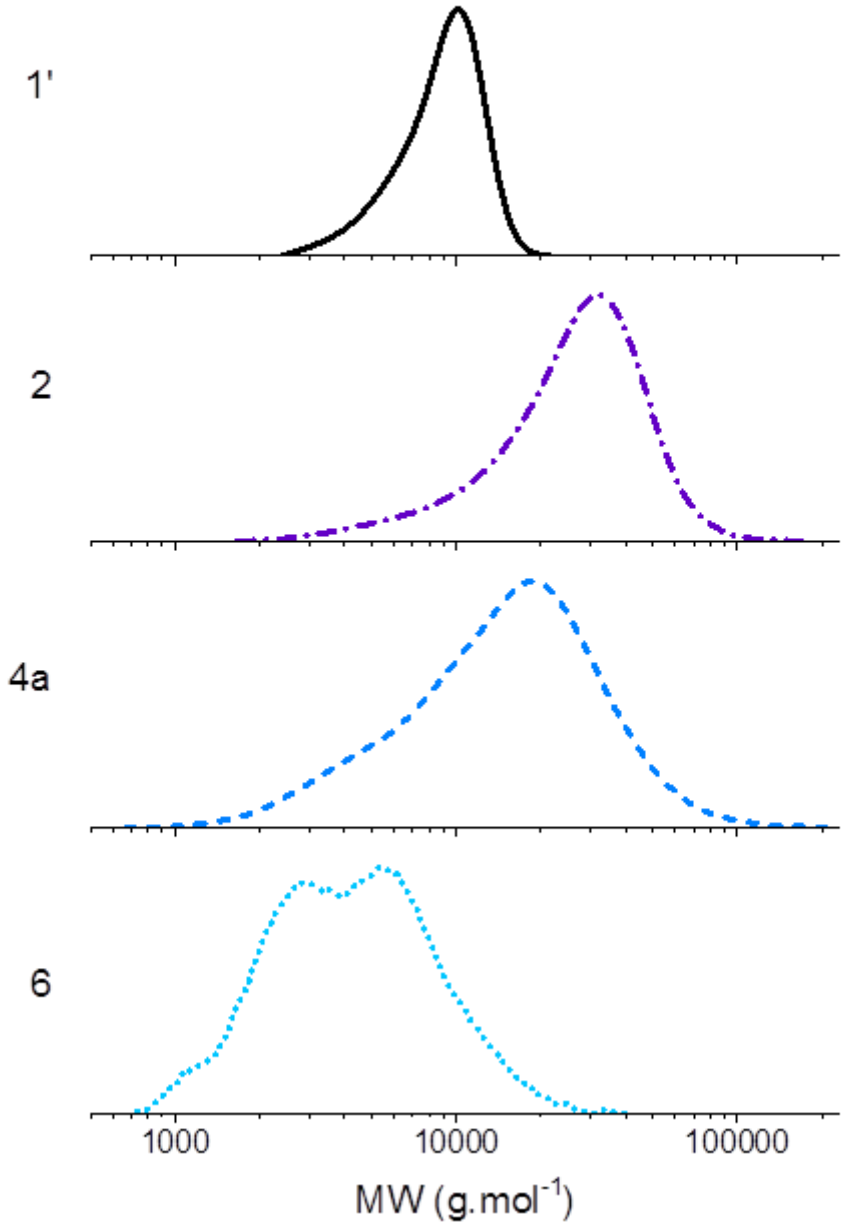

Figure S4. Molecular weight distribution obtained by SEC, using polystyrene calibration and THF as the eluent for the block copolymer precursor PLA_2 **(1')**, PTEGA-*b*-PLA_2 (**2**), purified product of the addition-elimination reaction (**4a**) with residual polylactide and the PLA precipitate (**6**).

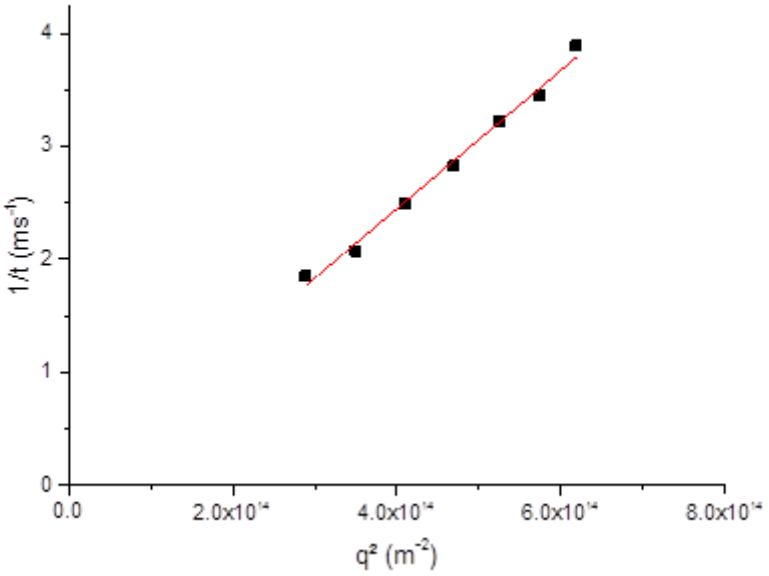

Figure S5. Plot of τ-1 vs. q^2 for micelles (1 mg.mL^{-1}), **3**.

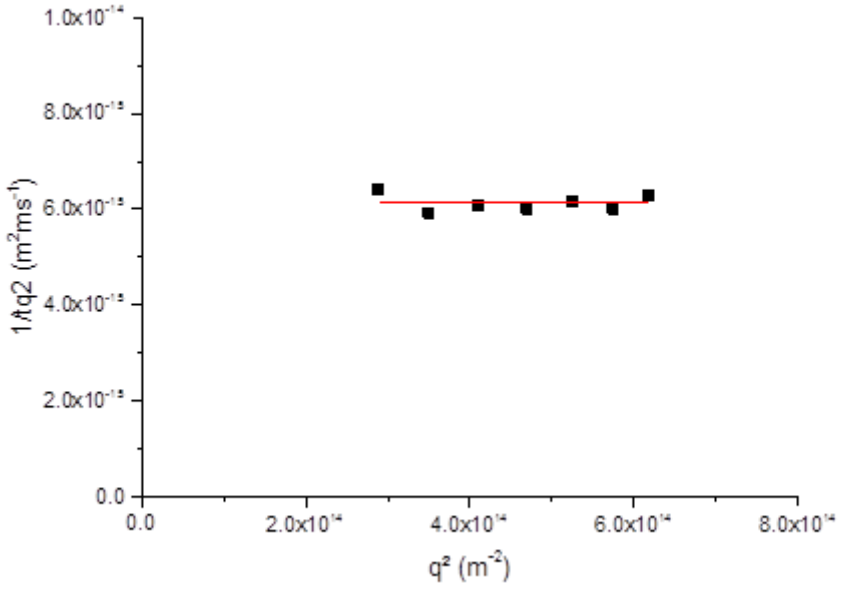

Figure S6. Plot of $\tau^{-1}q^{-2}$ *vs.* q^2 for micelles (1 mg.mL^{-1}), **3**.

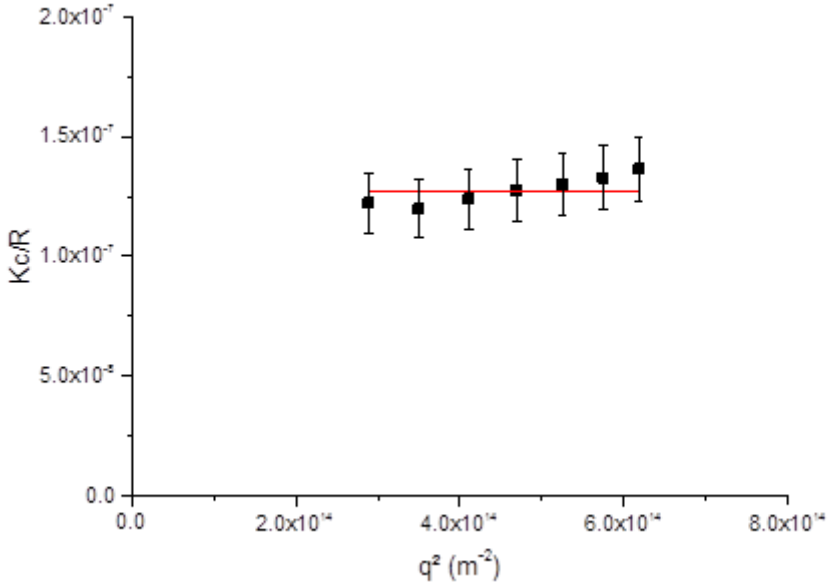

Figure S7. Plot of Kc/R *vs.* q^2 for micelles (1 mg.mL^{-1}), **3**.

Note for particles smaller than λ/20, only a negligible phase difference exists between light emitted from the various scattering centers within the given particle. In this case, the detected scattered intensity will be independent of the scattering angle and only depend on the mass of the particle which is proportional to the total number of scattering centers one particle contains.[11]

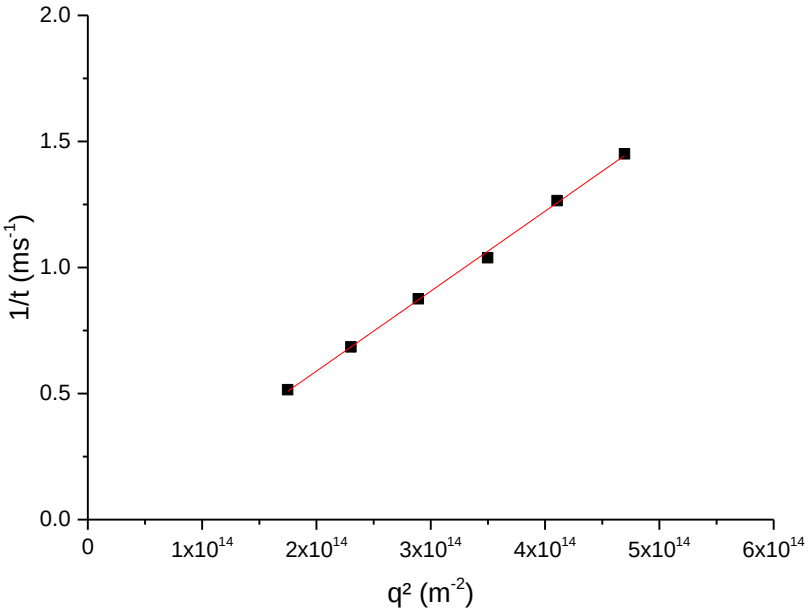

Figure S8. Plot of τ^{-1} *vs.* q^2 for the product, **4a** (2 mg.mL^{-1}), of the reaction of thiophenol with micelles, **3,** prior to centrifugation, drying and re-suspension.

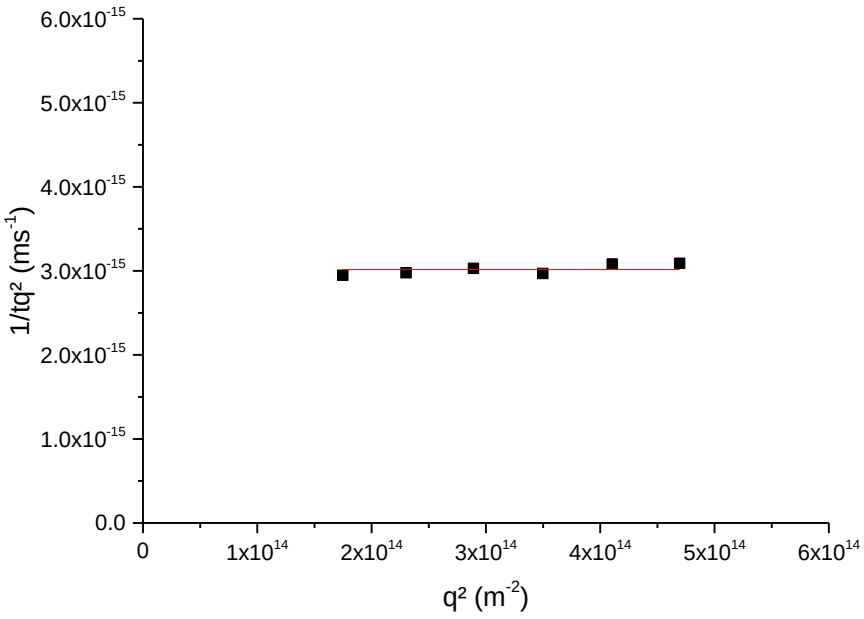

Figure S9. Plot of $\tau^{-1}q^{-2}$ *vs.* q^2 for the product, **4a** (2 mg.mL^{-1}), of the reaction of thiophenol with micelles, **3,** prior to centrifugation, drying and re-suspension.

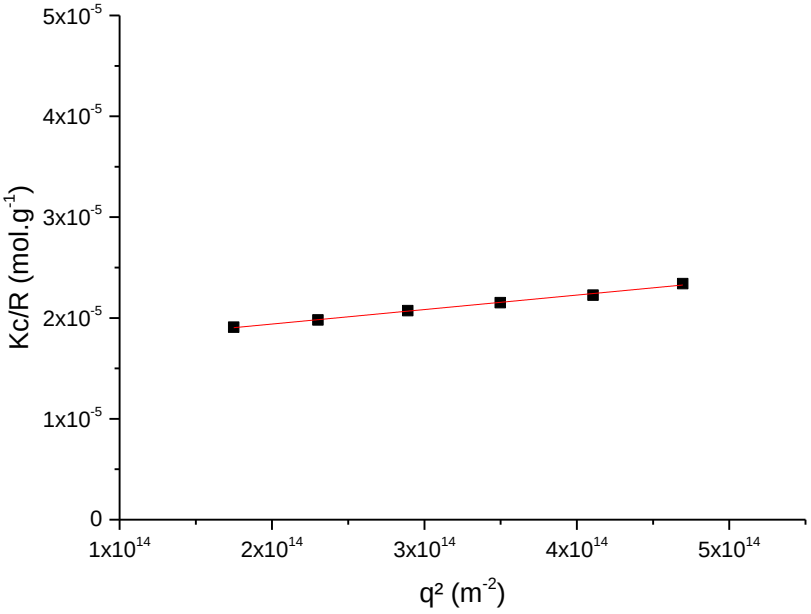

Figure S10. Plot of Kc/R *vs.* q² for the product, **4a** (2 mg.mL^{-1}), of the reaction of thiophenol with micelles, **3,** prior to centrifugation, drying and re-suspension.

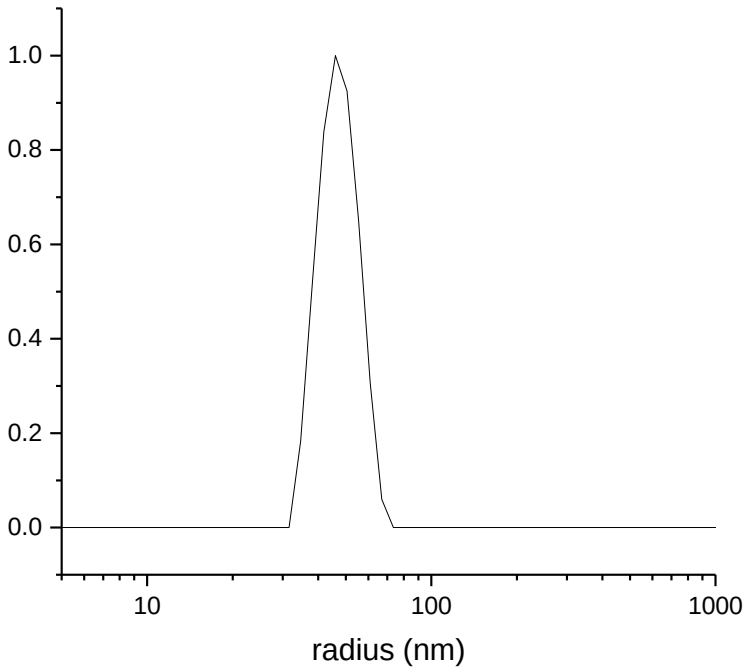

Figure S11. Size distribution for the nanostructure **4a** (2 mg.mL^{-1}) at 90°

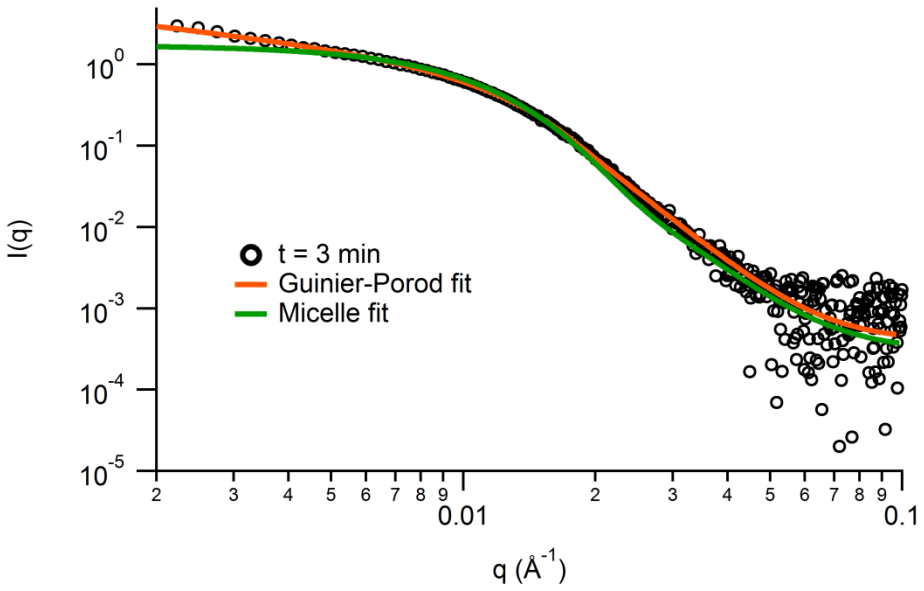

Figure S12. SAXS profile and fits for the reaction of **3** with thiophenol after 3 min. The Guinier-Porod fit gives a R_g value of 12 nm, such a difference with LS can be explained by the hydration of the PTEGA core, and thus the radius visible by SAXS corresponds to the radius of the core and a partial layer of the shell, the one which is more dense and near the core. Such an incomplete visibility of a hydrophilic corona has already been observed.[12, 13] The PolyCoreForm used for this fit is considered as a uniform micelle with some dispersity ($Đ$ = 0.3), a radius of 14 nm was obtained, which fits well with the R_g obtained with the Guinier-Porod plot. The scattering length density of the micelle was found slightly higher than usual for lactide, which suggests the incorporation of some PTEGA in this layer.

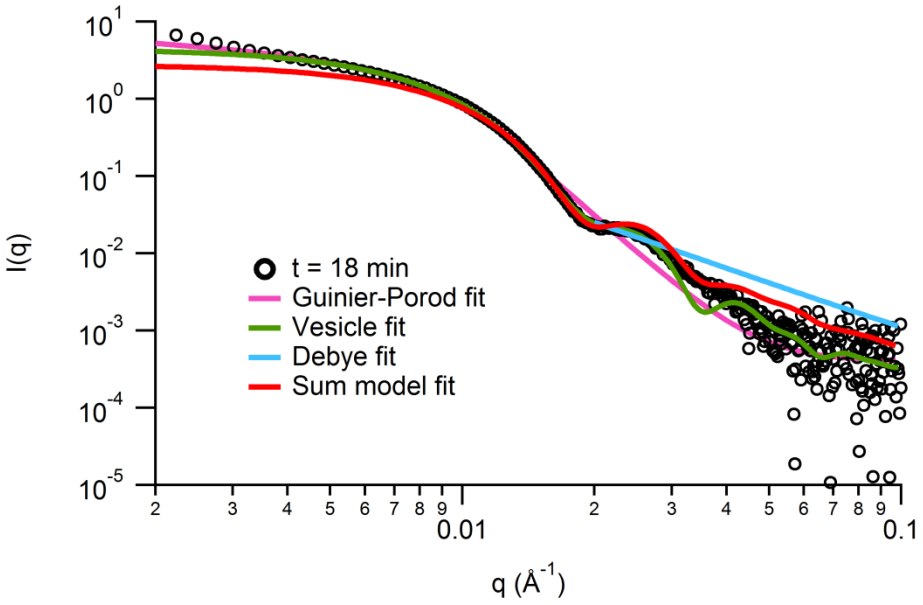

Figure S13. SAXS profile and fits for the reaction of **3** with thiophenol after 18 min. The Guinier-Porod fit gives a R_g value of 20 nm, which is lower than the value determined by LS. Again, the hydration of PTEGA does not allow for the polymer to be entirely visible by SAXS. A PolyCoreForm with a core-shell structure fit the experimental curvefor *q* values below 0.025 $Å^{-1}$, which suggests the presence of another morphology with poorly-defined form factor in the solution. This correlates well with the presence of polylactide in solution. Polylactide being hydrophobic, it tends to form collapsed coils in water, which was confirmed by a Debye fit. To further confirm the presence of these two structures in solution, a linear combination of the PolyCoreForm with a core-shell structure and Debye fits was performed. This Sum model confirms the structure of vesicles with a large dispersity on the core. These vesicles are seems as a core full of water with a radius of 4 nm and a shell of PTEGA with a thickness of 19 nm. These values are similar to the ones obtained with the PolyCoreForm fit for vesicle alone, and are in good agreement with the Guinier-Porod fit. The addition of random coil polymer allowed for a better fit for *q* values above 0.025 $Å^{-1}$.

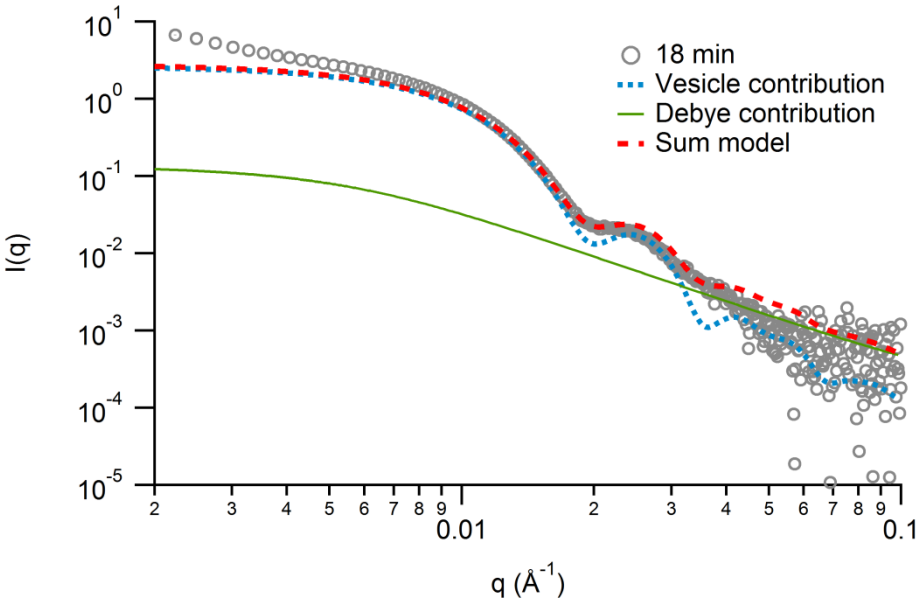

Figure S14. SAXS data after 18 minutes of reaction of **3** with thiophenol. The two components of the Sum model used previously are shown. The vesicle contribution is much more important at low q than the Debye one and for q above 0.015 Å, the two models contribute more equally.

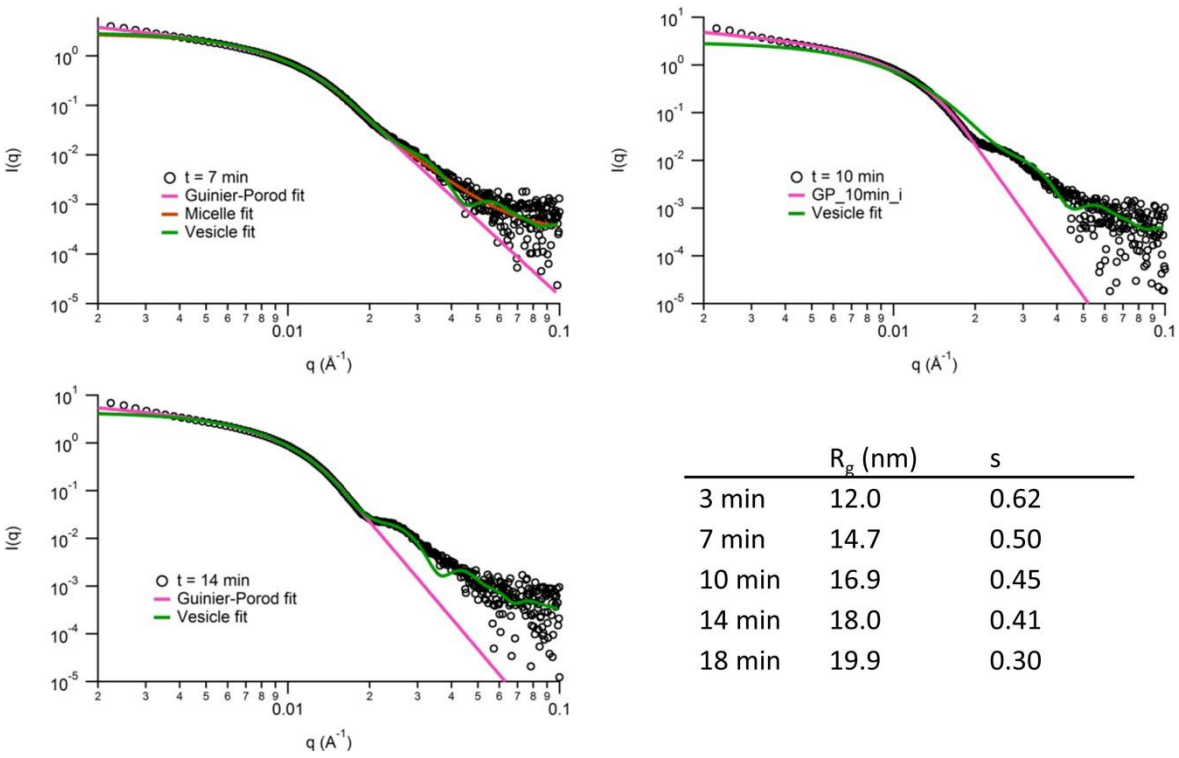

	R_g (nm)	s
3 min	12.0	0.62
7 min	14.7	0.50
10 min	16.9	0.45
14 min	18.0	0.41
18 min	19.9	0.30

Figure S15. SAXS curves and fits at different time point during the reaction of **3** with thiophenol. A Guinier-Porod used for each curve provides general information on the shape and size of the sample in solution (see values in Table). The values follow a trend: bigger particles are obtained after the reaction, and they are more spherical than at the beginning of the reaction. A transition from spherical micelle to vesicle is confirmed by the change of shape of the raw data curves and the poor fit provided by the micelle model after 7 min.

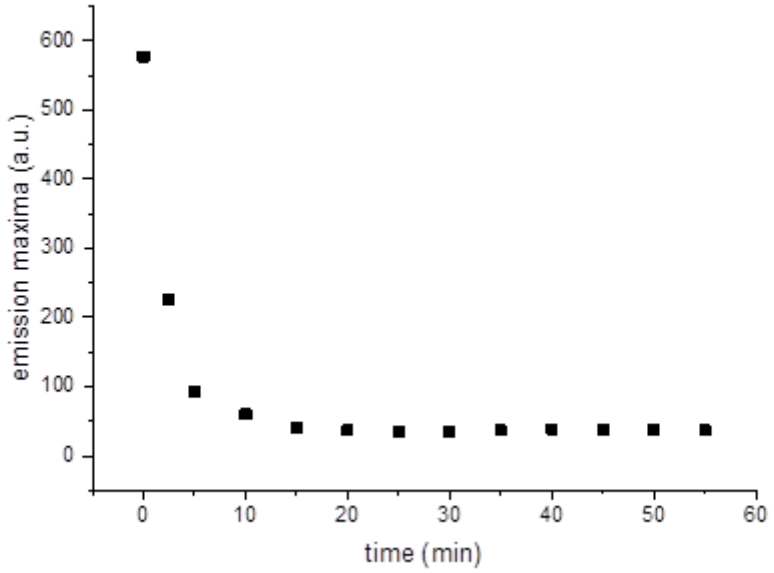

Figure S16. Variation of fluorescence emission maxima at 510 nm over time after addition of thiophenol to micelles, **3**. Excitation wavelength 405 nm.

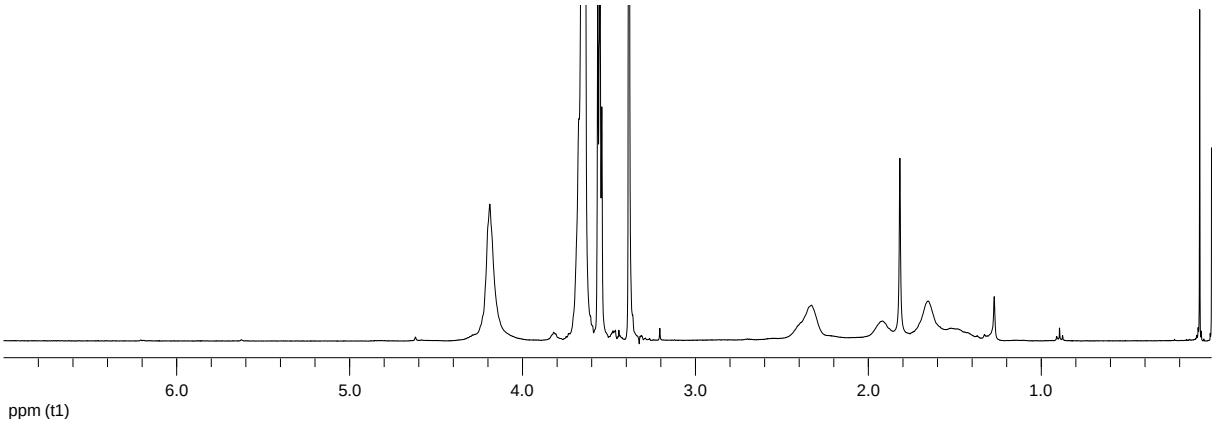

Figure S17. ^{1}H NMR (400 MHz, $CDCl_3$) spectrum of PTEGA, **5**.

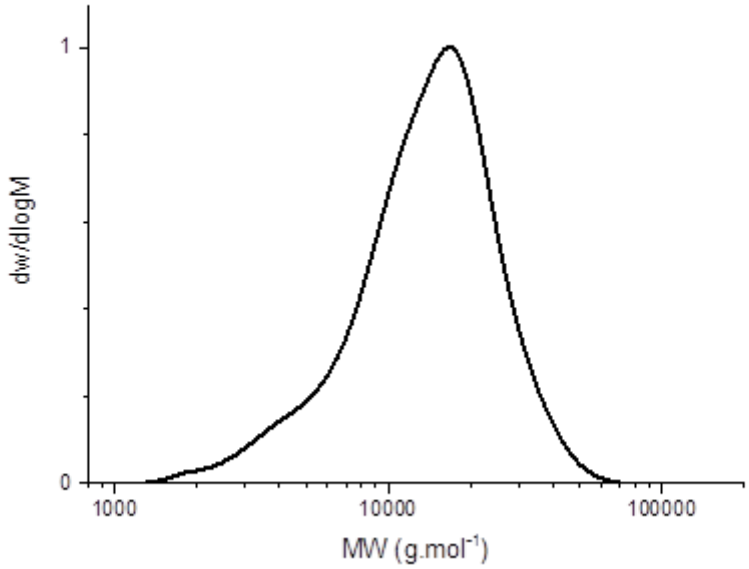

Figure S18. Molecular weight distribution obtained by SEC, using polystyrene calibration and THF as the eluent for the homopolymer PTEGA, **5**.

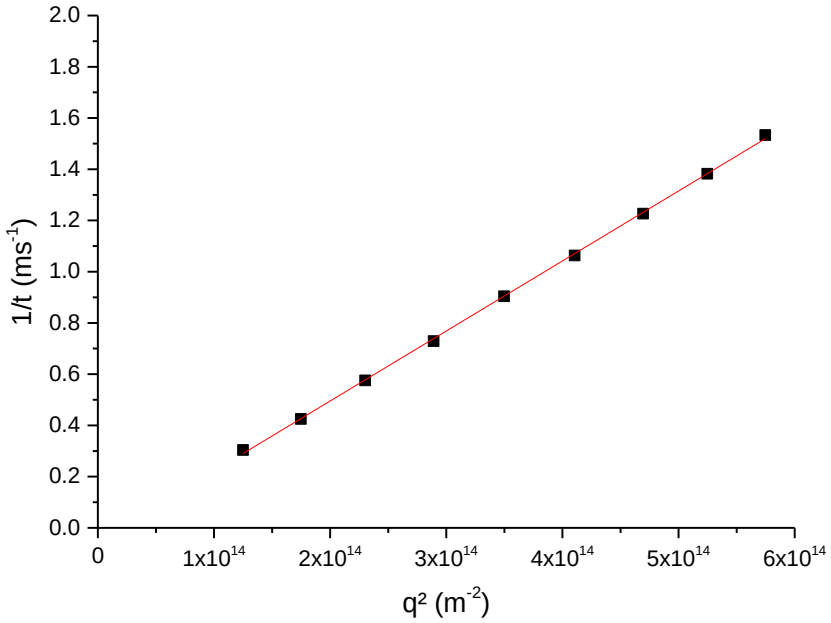

Figure S19. Plot of τ^{-1} *vs.* q^2 for the product, **4b** (2 mg.mL^{-1}), of the reaction of thiophenol with homopolymer, **5**.

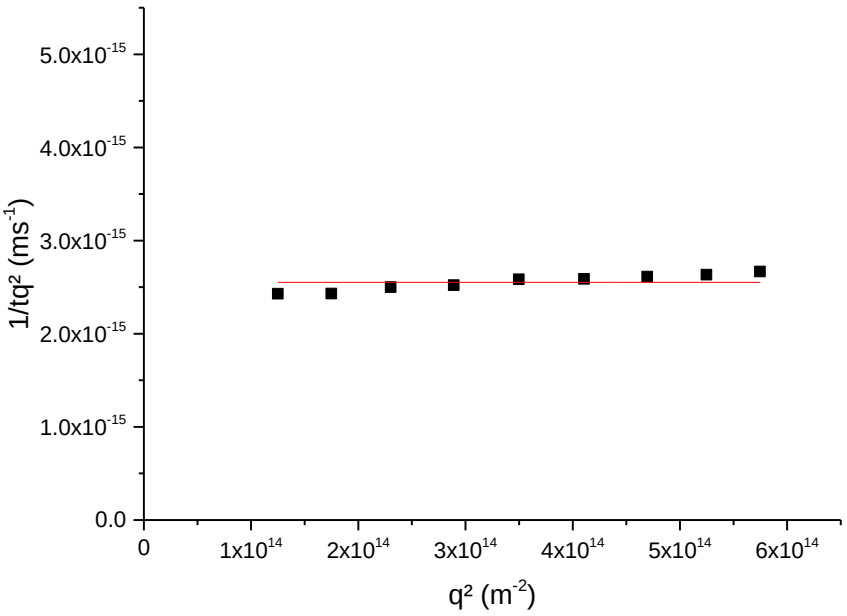

Figure S20. Plot of $\tau^{-1}q^{-2}$ *vs.* q^2 for the product, **4b** (2 mg.mL^{-1}), of the reaction of thiophenol with homopolymer, **5**.

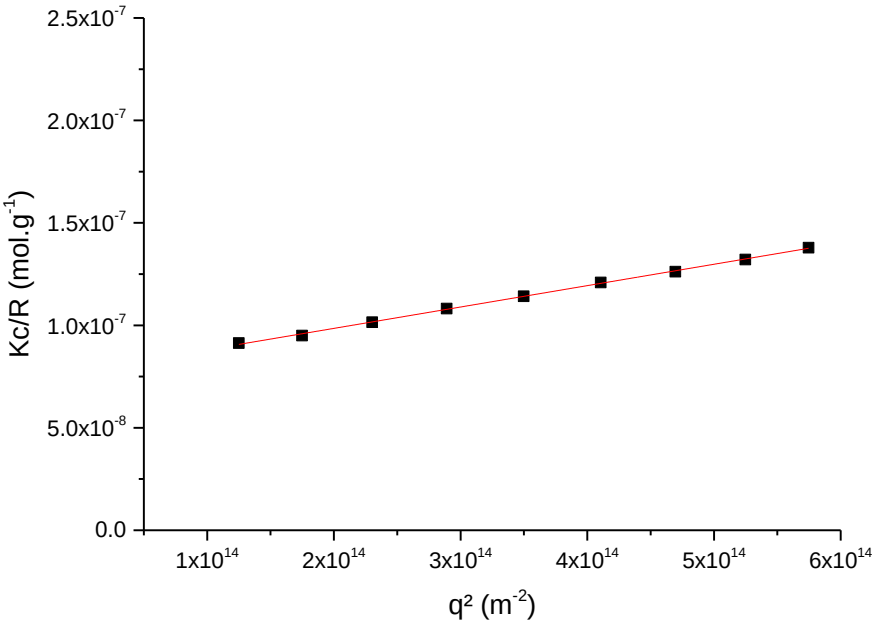

Figure S21. Plot of Kc/R *vs.* q² for the product, **4b** (2 mg.mL^{-1}), of the reaction of thiophenol with homopolymer, **5**.

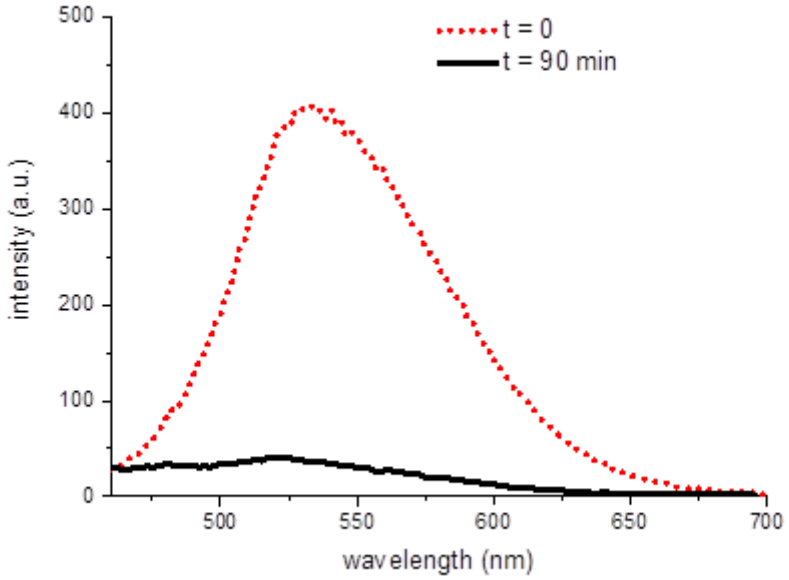

Figure S22. Fluorescence emission spectra for the addition-elimination reaction of homopolymer (**5**) with thiophenol, before the reaction (dotted line) and after the reaction (solid line) solution **4b**. Emission maxima at 535 nm with an excitation wavelength of 415 nm.

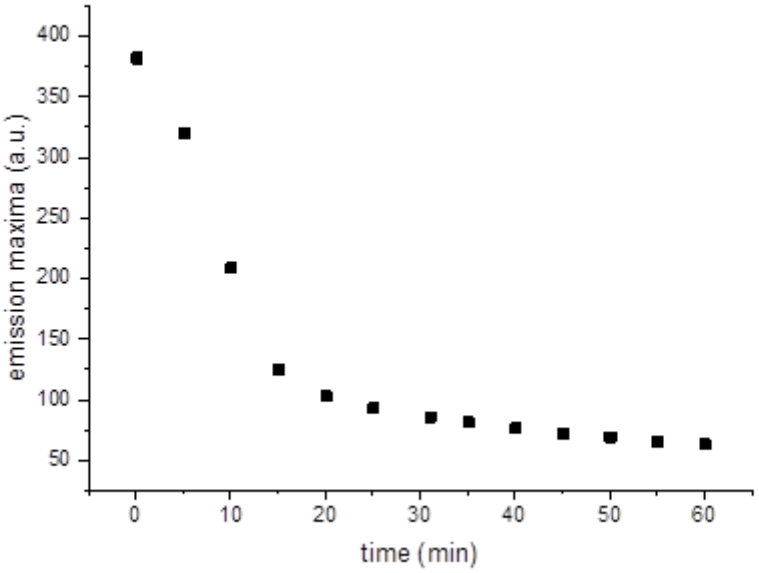

Figure S23. Variation of fluorescence emission maxima at 535 nm over time after addition of thiophenol to the homopolymer, **5**. Excitation wavelength 415 nm.

References

1. F. Hua, X. Jiang, D. Li and B. Zhao, *J Polym Sci, Part A: Polym Chem*, 2006, **44**, 2454-2467.
2. M. P. Robin, P. Wilson, A. B. Mabire, J. K. Kiviaho, J. E. Raymond, D. M. Haddleton and R. K. O'Reilly, *J Am Chem Soc*, 2013, **135**, 2875-2878.
3. M. P. Robin, A. B. Mabire, J. C. Damborsky, E. S. Thom, U. H. Winzer-Serhan, J. E. Raymond and R. K. O'Reilly, *J Am Chem Soc*, 2013, **135**, 9518-9524.
4. A. Guinier and G. Fournet, *Small-angle scattering of X-Rays*, John Wiley & Sons, New York, 1955.
5. O. Glatter and O. Kratky, *Small-Angle X-Ray Scattering*, Academic Press, 1982.
6. R.-J. Roe, *Methods of X-ray and Neutron Scattering in Polymer Science*, Oxford University Press, New York, 2000.
7. P. Bartlett and R. H. Ottewill, *J Chem Phys*, 1992, **96**, 3306-3318.
8. S. T. Mudie, *scatterBrain*, (2013), Australian Synchrotron.
9. S. Kline, *J Appl Crystallogr*, 2006, **39**, 895-900.
10. NIST SLD calculator.
11. J. P. Patterson, M. P. Robin, C. Chassenieux, O. Colombani and R. K. O'Reilly, *Chem Soc Rev*, 2014, **43**, 2412-2425.
12. A. Pitto-Barry, N. Kirby, A. P. Dove and R. K. O'Reilly, *Polym Chem*, 2014, **5**, 1427-1436.
13. L. Sun, N. Petzetakis, A. Pitto-Barry, T. L. Schiller, N. Kirby, D. J. Keddie, B. J. Boyd, R. K. O'Reilly and A. P. Dove, *Macromolecules*, 2013, **46**, 9074-9082.